**Beam Systematics for Mott Experiment Runs I and II**

Joe Grames and Brian Freeman

February 22, 2017

JLab-TN-17-007

# 1 Introduction

Systematic studies of the Mott experimental asymmetry to electron beam conditions such as beam position, beam size, and energy spread were measured during Runs I and II. The beam conditions are analyzed and summarized in this note. A simple schematic of the relevant beam components is shown in Fig. 1.

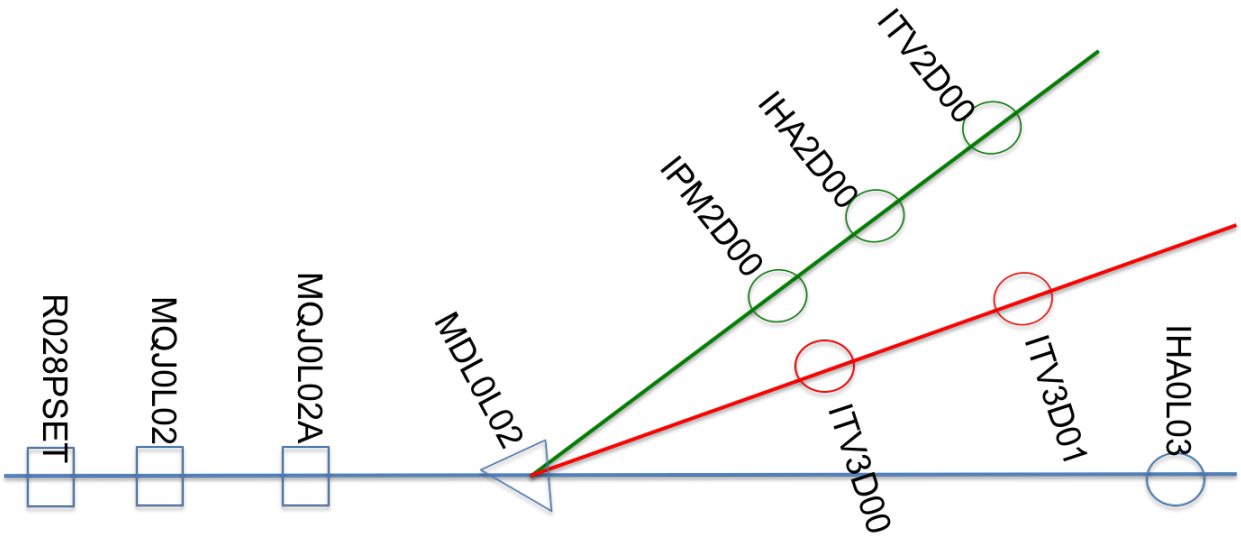


Fig. 1. Schematic shows relative location of elements; the dipole magnet sends beam to the Mott (red) or spectrometer (green) beam lines. Quads MQJ0L02/MQJ0L02A control beam size and SRF cavity phase R028PSEt controls energy spread. Wire scanners IHA0L03 and IHA2D00 are used to measure beam emittance/Twiss at MQJ0L02 and momentum spread, respectively.

# 2 Elegant Model

An Elegant model of the layout in Fig. 1 was constructed beginning at MQJ0L02 and ending at either IHA2D00 or ITV3D00. The lattice is listed here:

```
"cle" ! clear whole RPN stack for safety

% 1 atan 4 * sto pi
% pi 180 / sto cdtor
% 180 pi / sto crtod

! DRIFT BETWEEN QUADS
D1      : DRIFT, L=0.4596
```

```
! DRIFT TO 2D LINE
D2        : DRIFT, L=1.0065
D3        : DRIFT, L=3.1385
D4        : DRIFT, L=0.1778
D5        : DRIFT, L=0.1270

! DRIFT TO 3DLINE
D6        : DRIFT, L=1.0041
D7        : DRIFT, L=0.5584
D8        : DRIFT, L=0.2667
D9        : DRIFT, L=0.8113

! NORMAL MOTT
MQJ0L02:  KQUAD, L=0.15, K1= -5.04003396226415
MQJ0L02A: KQUAD, L=0.15, K1= +5.00232327044025

! 2D DIPOLE
MDL0L02_2D: CSBEND, L=0.1230, ANGLE="-30.0 180.0 / -1 acos * ", &
         E1=" 0.0 180.0 / -1 acos * ", E2="-30.0 180.0 / -1 acos * ", &
         EDGE_ORDER=2, HGAP=0.013564, FINT=0.5, NONLINEAR=1, &
         N_KICKS=15, INTEGRATION_ORDER=4

! 3D DIPOLE
MDL0L02_3D: CSBEND, L=0.1278, ANGLE="-12.5 180.0 / -1 acos * ", &
         E1=" 0.0 180.0 / -1 acos * ", E2="-12.5 180.0 / -1 acos * ", &
         EDGE_ORDER=2, HGAP=0.013564, FINT=0.5, NONLINEAR=1, &
         N_KICKS=15, INTEGRATION_ORDER=4

! DIAGNOSTIC IN 2D LINE
IPM2D00: WATCH, FILENAME="%s.ITV2D00", MODE=COORD
ITV2D00: WATCH, FILENAME="%s.ITV2D00", MODE=COORD
IHA2D00: WATCH, FILENAME="%s.IHA2D00", MODE=COORD

! DIAGNOSTIC IN 3D LINE
ITV3D00: WATCH, FILENAME="%s.ITV3D00", MODE=COORD
ITV3D01: WATCH, FILENAME="%s.ITV3D00", MODE=COORD

! BEAM LINES
2D:  LINE=(MQJ0L02, D1, MQJ0L02A, D2, MDL0L02_2D, D3, IPM2D00, D4,
IHA2D00, D5, ITV2D00)
3D:  LINE=(MQJ0L02, D1, MQJ0L02A, D6, MDL0L02_3D, D7, D8, ITV3D00, D9,
ITV3D01)
```

The horizontal dispersion function is calculated at the spectrometer harp IHA2D00 $\eta_x$ = -1.946 m and at the Mott target foil ITV3D01 $\eta_x$ = -0.3767 m.

# 3 Run I Results

### Run I Energy

The electron beam kinetic energy reported in [1] is 4.806 ± 0.097 MeV. This corresponds to a total energy of 5.317 ± 0.097 MeV and a momentum of 5.292 ± 0.098 MeV/c.

**Run I Beam Emittance**

The beam emittance is determined by a quad – drift – profile measurement. Quadrupole MQJ0L02 was scanned over strengths to observe waists in both horizontal and vertical projections at harp IHA0L03. Measurements made on two subsequent days using *qsUtility 3.21* with similar ranges of quad strength are analyzed and reported in e3458895. Plots of the beam size vs. geometric quad strength are shown in Fig. 2. Corresponding emittance and Twiss parameters calculated by *sddsemitproc* at MQJ0L02 are summarized in Table 1.

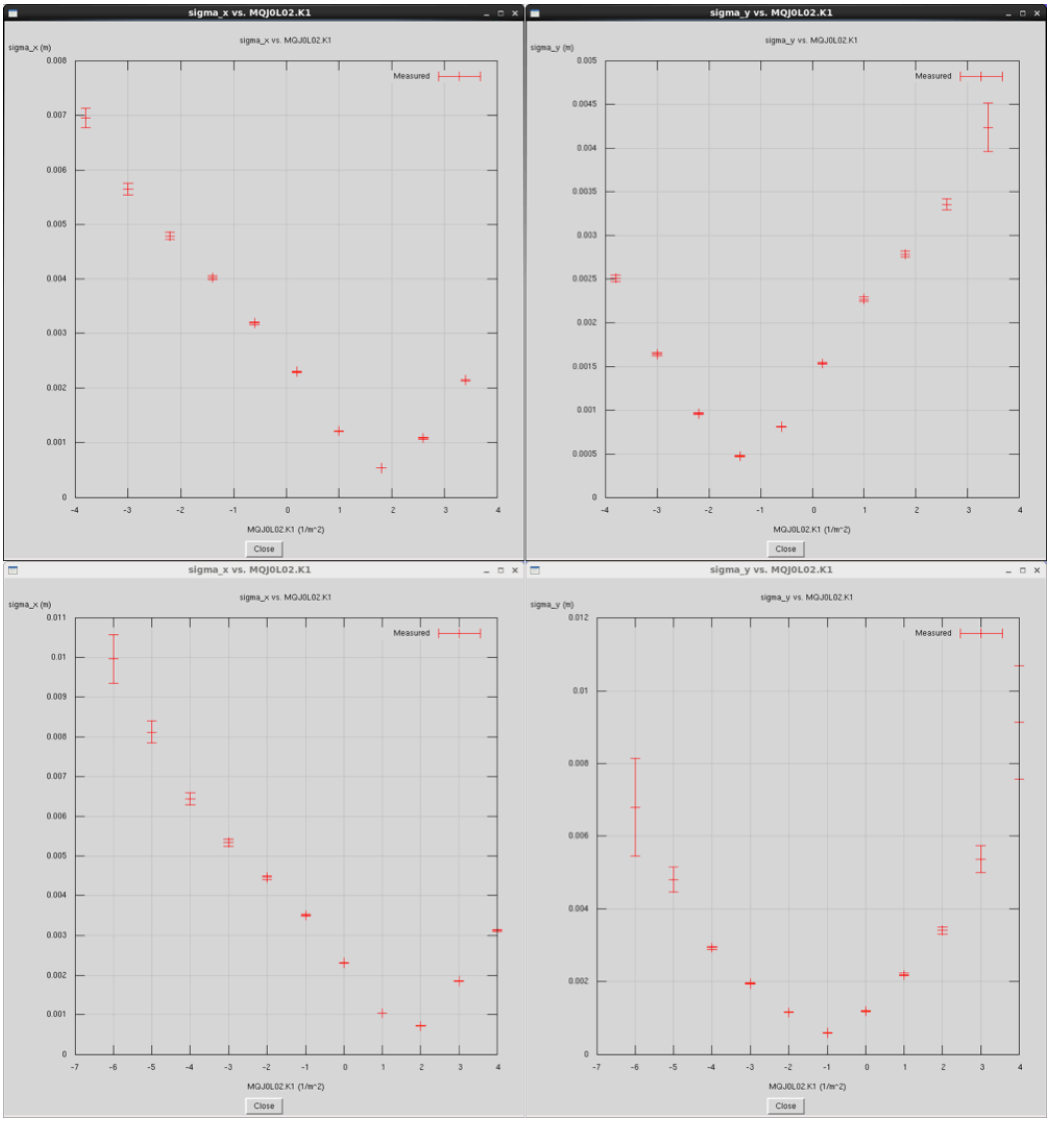


Fig. 2. Upper (lower) plots show plots of beam size measured at IHA0L03 as a function of quad strength MQJ0L02 taken at 2015-01-18_22:36 (IHA0L03_2015-01-19_17:15).

Table 1. Summary of measured normalized emittance and Twiss parameters at MQJ0L02.

| qsUtility (run date) | $\varepsilon_{n,x}$ (μm) | $\beta_x$ (m) | $\alpha_x$ (rad) | $\varepsilon_{n,y}$ (μm) | $\beta_y$ (m) | $\alpha_y$ (rad) |
|---|---|---|---|---|---|---|
| 2015-01-18_22:36 | 1.077(2) | 15.39(5) | -1.985(06) | 0.683(43) | 13.25(12) | -0.612(12) |
| 2015-01-19_17:15 | 1.206(5) | 14.08(1) | -1.389(17) | 0.930(66) | 11.06(09) | -0.065(10) |

**Run I Beam Energy Spread Measurements**

The Mott asymmetry was studied as a function of energy spread by varying the phase setting R028PSET of the second QCM SRF cavity about the nominal Run 1 operating set point. The beam energy spread is determined from a measurement of the beam size at a dispersive location according to

$$(S_x)^2 = \varepsilon_x \beta_x + (\frac{dp}{p} x\ \eta_x)^2$$

where $S_x$ is the horizontal beam size. For each case the beam was sent to the spectrometer wire scanner IHA2D00 to measure the beam size and then to Mott target #15 (1um gold) to measure the asymmetry with the IHWP both IN and OUT. The cavity gradient and a steering coil were used to adjusted small amounts as shown in Table 2. The horizontal beam size is determined by a fit of the scanner profile.

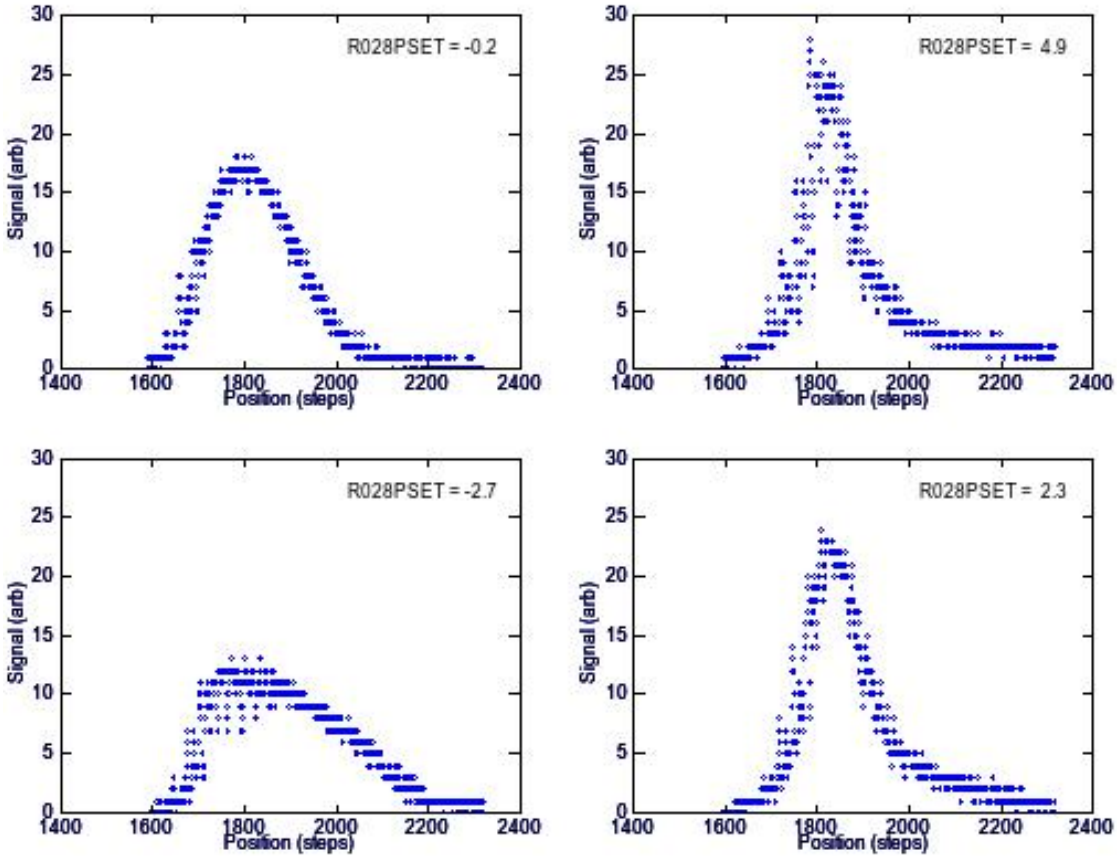


Fig. 3. Plots shows horizontal wire scanner signal as a function of motor potentiometer position with a conversion of 0.02041 mm/step.

Table 2. Parameters and results of energy spread measurements.

| R028-PSET | Δ-PSET | R028 GSET | MAD 3D00H | IHWP IN | IHWP OUT | Harp File | $S_x$ (RMS) | | δp/p | δT |
|---|---|---|---|---|---|---|---|---|---|---|
| deg | deg | MV/m | G-cm | Mott | Mott | Prefix = IHA2D00_ | steps | mm | $10^{-3}$ | (keV) |
| -0.2 | 0.0 | 4.81 | 0 | 8180 | 8181 | 2015-01-19_22:55 | 107.48 | 2.19 | 1.117 | 4.897 |
| 4.8 | -5.0 | 4.82 | 20 | 8182 | 8183 | 2015-01-19_22:44 | 136.29 | 2.78 | 1.421 | 6.232 |
| -2.7 | 2.5 | 4.81 | -9 | 8184 | 8185 | 2015-01-19_22:53 | 137.63 | 2.81 | 1.435 | 6.293 |
| 2.3 | -2.5 | 4.81 | 11 | 8186 | 8187 | 2015-01-19_22:51 | 118.55 | 2.42 | 1.234 | 5.410 |

Applying the emittance results (2015-01-19_17:15) collected prior to the energy spread measurement and the corresponding quad values MQJ0L02 = -133.65 G (K = -5.048 $m^{-1}$) and MQJ0L02A = 132.95 G (K = 5.010 $m^{-1}$) the beam size without dispersive effects at harp IHA2D00 is 0.3001 mm. Consequently, the relative momentum spread (δp/p) and energy spread (δT) are computed and are shown in Table 2 and plotted in Fig. 4 The relatively low value (compared to usual CEBAF operation) is indicative of running the injector for conditions to minimize energy spread.

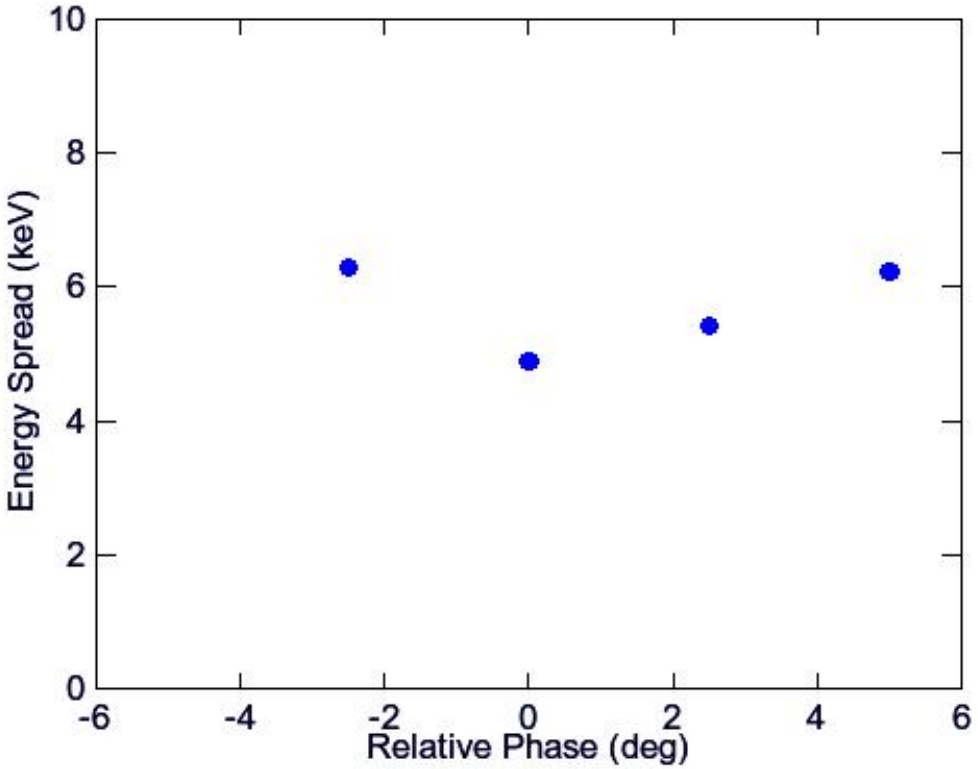


Fig. 3. The computed energy spread as a function of relative phase of second SRF cavity about the value used for Run 1 (R028PSET = -0.2 deg).

**Run I Beam Spot Size**

The Mott asymmetry was studied as a function of beam spot size on foil #15 (1μm gold) with about 2 μA of beam current. Spot size was controlled using the quad values for MQJ0L02 and MQJ0L02A about their nominal Run 1 operating set points. The spot size at the target predicted with Elegant using the quad values, corresponding emittance (2015-01-19_17:15) and relative momentum spread ($1.117 \times 10^{-3}$) is in Table 1.

Table 3. Parameters and results of spot size measurements. "Name" corresponds to the beam size we expected during Run 1 (in millimeters) and "Fig." is the label for the corresponding OTR foil image in e3318205.

| Name | Fig. | MQJ0L02 | | MQJ0L02A | | IHWP IN | IHWP OUT | Sx | Sy |
|---|---|---|---|---|---|---|---|---|---|
| | | G | 1/m | G | 1/m | | | mm | mm |
| 0.100 | 1 | -133.00 | -5.0231 | 153.00 | 5.7785 | 8163 | 8164 | 0.57 | 0.42 |
| 0.250 | 2 | -115.00 | -4.3433 | 139.00 | 5.2497 | 8165 | 8166 | 0.67 | 0.33 |
| 0.500 | 3 | -164.00 | -6.1939 | 153.00 | 5.7785 | 8167 | 8169 | 0.93 | 0.95 |
| 1.000 | 4 | -188.00 | -7.1003 | 141.00 | 5.3252 | 8170 | 8171 | 1.65 | 1.47 |
| 2.000 | 5,6 | -264.00 | -9.9707 | 130.00 | 4.9098 | 8172 | 8173 | 3.29 | 2.96 |
| 0.750 | 7 | -182.00 | -6.8737 | 148.00 | 5.5896 | 8174 | 8175 | 1.33 | 1.33 |
| 1.500 | 8,9 | -225.00 | -8.4977 | 135.00 | 5.0986 | 8176 | 8177 | 2.45 | 2.21 |
| 0.475 | 10 | -133.65 | -5.0477 | 132.65 | 5.0099 | 8178 | 8179 | 1.08 | 0.53 |

**Run I Beam Position Study**

The Mott asymmetry was studied as a function of beam position two targets; foil #15 (1μm gold) e3318095 with about 2 μA and foil #1 (0.225 μm gold) e3318137 with about 4 μA. Position was controlled using far-upstream steering coils MBH0L01AH and MBH0L01AV. The beam was moved to 6 locations about the nominal position for Run 1, corresponding to a total of 7 positions per foil. The beam position at the target is calculated using saved camera images of the OTR emitted from the foils.

Three steps are required to determine the OTR position at the foil from the logbook camera images:

- the raw PNG image files are processed with ImageJ to determine a fixed bounding box of 165 x 165 pixels centered on each image within 2 px, and the centroid of each OTR profile is computed in the reference frame of the camera

- the reference frame of the camera is transformed to the reference frame of the target foil by considering a) camera is mounted approximately 45° on vacuum chamber facing internal mirror resulting in coupled axes, b) mirror faces target ladder at approximately 13° from beam axis resulting in subtended view of target ladder, c) mirror inverts image about the vertical target axis. The transformation between camera pixels and beam pixels is given by (see Appendix A for details):

$$\begin{pmatrix} x_b \\ y_b \end{pmatrix} = \begin{pmatrix} -0.579 & -0.579 \\ -1.000 & 0.707 \end{pmatrix} \begin{pmatrix} x_p \\ y_p \end{pmatrix}$$

  - the surveyed target ladder calibrations (steps/mm) are used to calibrate pixel distance of transformed images using images of known step size displacement.

Table 4. Summary of position measurements.

| Foil | Motion | | MBH0L01A Absolute | | MBH0L01A Relative | | Image | Mott Run | | Foil Rel (mm) | | |
|---|---|---|---|---|---|---|---|---|---|---|---|---|
| | Real | OTR | H | V | H | V | | IN | OUT | X | Y | R |
| 15 | 0 | 0 | -70.7 | -30.9 | 0 | 0 | run1-foil15-fig7.png | 8132 | 8131 | 0.0 | 0.0 | 0.0 |
| 15 | U | U | -70.7 | -0.9 | 0 | 30 | run1-foil15-fig5.png | 8134 | 8133 | 0.1 | 0.7 | 0.7 |
| 15 | D | D | -70.9 | -60.9 | -0.2 | -30 | run1-foil15-fig6.png | 8136 | 8135 | 0.0 | -0.8 | 0.8 |
| 15 | R | L | -40.9 | -30.9 | 29.8 | 0 | run1-foil15-fig8.png | 8138 | 8137 | 0.5 | 0.1 | 0.5 |
| 15 | L | R | -100.7 | -30.9 | -30 | 0 | run1-foil15-fig9.png | 8140 | 8139 | -0.6 | -0.1 | 0.6 |
| 15 | LD | RD | -100.7 | -60.9 | -30 | -30 | run1-foil15-fig10.png | 8142 | 8141 | -0.6 | -0.8 | 1.0 |
| 15 | RU | LU | -40.7 | -0.9 | 30 | 30 | run1-foil15-fig11.png | 8144 | 8143 | 0.5 | 0.9 | 1.1 |
| 1 | 0 | 0 | -70.7 | -30.9 | 0 | 0 | run1-foil1-fig3.png | 8146 | 8145 | 0.0 | 0.0 | 0.0 |
| 1 | LD | RD | -100.7 | -60.9 | -30 | -30 | run1-foil1-fig4.png | 8149 | 8147 | -0.6 | -0.9 | 1.1 |
| 1 | LU | RU | -100.7 | -0.9 | -30 | 30 | run1-foil1-fig5.png | 8151 | 8150 | -0.5 | 0.6 | 0.8 |
| 1 | RU | LU | -40.7 | -0.9 | 30 | 30 | run1-foil1-fig6.png | 8153 | 8152 | 0.5 | 0.9 | 1.1 |
| 1 | RD | LD | -40.7 | -60.9 | 30 | -30 | run1-foil1-fig8.png | 8155 | 8154 | 0.6 | -0.6 | 0.8 |
| 1 | D | D | -70.7 | -60.9 | 0 | -30 | run1-foil1-fig9.png | 8157 | 8156 | 0.0 | -0.7 | 0.7 |
| 1 | L | R | -100.7 | -30.9 | -30 | 0 | run1-foil1-fig10.png | 8159 | 8158 | -0.5 | -0.2 | 0.5 |

# 4 Run II Results

### Run II Energy

The electron beam kinetic energies for Run II reported in [1] are shown in Table 5 alongside the corresponding Mott runs.

Table 5. Run II Beam Momentum and Kinetic Energy

| R028 | Momentum | | Kinetic Energy | | Mott Runs | | Mott Runs | |
|---|---|---|---|---|---|---|---|---|
| GSET | P | δP | T | δT | Foil #15 (1 μm) | | Foil #14 (0.35 μm) | |
| MV/m | MeV/c | MeV/c | MeV | MeV | In | Out | In | Out |
| 3.350 | 5.025 | 0.012 | 4.540 | 0.012 | 8457<br>8459 | 8458<br>8460 | 8462<br>8464 | 8461<br>8463 |
| 3.740 | 5.219 | 0.013 | 4.733 | 0.012 | 8445<br>8447 | 8446<br>8448 | 8450<br>8452 | 8449<br>8451 |
| 4.120 | 5.404 | 0.013 | 4.917 | 0.013 | 8433<br>8435 | 8434<br>8436 | 8438<br>8440 | 8437<br>8439 |
| 4.500 | 5.603 | 0.013 | 5.115 | 0.013 | 8466<br>8469 | 8467<br>8470 | 8473<br>8475 | 8471<br>8474 |
| 4.890 | 5.785 | 0.014 | 5.297 | 0.014 | 8477<br>8479 | 8478<br>8480 | 8482<br>8484 | 8481<br>8483 |

# 5 Reference

1. J. Grames, "*Mott Experiment Run I/II Beam Energies*", JLAB-TN-17-001 (2017).

# 6 Appendix A

Step 1.

The ELOG entry images were saved as PNG files and cropped to 165 x 165 pixels. An example is shown here and summarized for all images below.

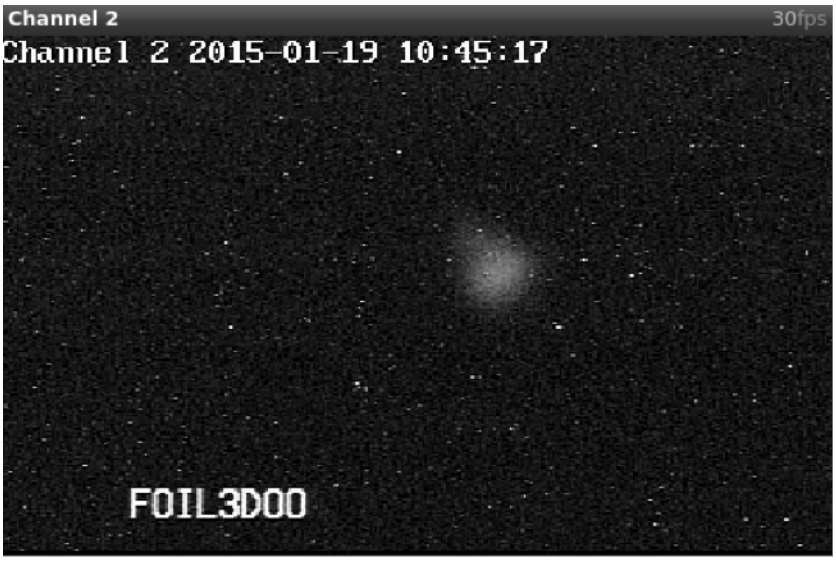


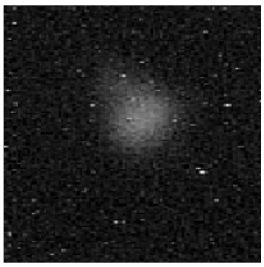

| FILENAME | WIDTH | HEIGHT | CEN_X | SIG_X | FWHM_X | CEN_Y | SIG_Y | FWHM_Y |
|---|---|---|---|---|---|---|---|---|
| run1-foil15-fig10.png | 165 | 165 | 114.5 | 12.9 | 30.5 | 95.2 | 18.6 | 43.9 |
| run1-foil15-fig11.png | 165 | 165 | 46.4 | 13.2 | 31.0 | 97.0 | 12.0 | 28.2 |
| run1-foil15-fig1.png | 165 | 165 | 47.2 | 13.8 | 32.6 | 117.7 | 14.5 | 34.2 |
| run1-foil15-fig5.png | 165 | 165 | 61.9 | 12.5 | 29.5 | 107.5 | 19.0 | 44.7 |
| run1-foil15-fig6.png | 165 | 165 | 99.4 | 13.2 | 31.0 | 75.8 | 14.1 | 33.3 |
| run1-foil15-fig7.png | 165 | 165 | 80.2 | 13.8 | 32.4 | 93.2 | 13.8 | 32.6 |
| run1-foil15-fig8.png | 165 | 165 | 65.2 | 13.9 | 32.6 | 78.6 | 16.4 | 38.6 |
| run1-foil15-fig9.png | 165 | 165 | 97.4 | 12.9 | 30.4 | 109.8 | 16.4 | 38.7 |
| run1-foil1-fig10.png | 165 | 165 | 101.7 | 15.3 | 36.0 | 106.8 | 17.4 | 40.9 |
| run1-foil1-fig3.png | 165 | 165 | 86.0 | 14.7 | 34.6 | 95.4 | 15.4 | 36.4 |
| run1-foil1-fig4.png | 165 | 165 | 121.2 | 15.3 | 35.9 | 92.8 | 16.5 | 38.9 |
| run1-foil1-fig5.png | 165 | 165 | 83.7 | 15.4 | 36.4 | 125.2 | 18.9 | 44.4 |
| run1-foil1-fig6.png | 165 | 165 | 52.1 | 15.6 | 36.7 | 99.4 | 14.5 | 34.2 |
| run1-foil1-fig8.png | 165 | 165 | 86.2 | 14.2 | 33.5 | 62.6 | 14.7 | 34.6 |
| run1-foil1-fig9.png | 165 | 165 | 102.4 | 14.4 | 34.0 | 78.8 | 17.6 | 41.6 |

Step 2.

The true beam position at the target is reduced in the plane of the target-mirror-camera by the projected distance of the mirror-foil vector relative to the beam axis. This value is estimated from drawings to be 13° from drawings however actual alignment of the mirror and its support fixture may result in a variation by as much as ±6°. This sub-tended image is collected along a target-mirror-camera plane of about 45° cw with respect the horizontal beam plane and is thus coupled. The image is also inverted by the mirror. Finally, the true beam position ($x_b$,$y_b$) is related to the camera pixel position ($x_p$,$y_p$) by the following transformation:

$$\begin{pmatrix} x_p \\ y_p \end{pmatrix} = \begin{pmatrix} -1 & 0 \\ 0 & 1 \end{pmatrix}_{Inv} \begin{pmatrix} \cos\phi & -\sin\phi \\ \sin\phi & \cos\phi \end{pmatrix}_{\phi=-45^\circ} \begin{pmatrix} \frac{1}{\cos\theta} & 0 \\ 0 & 1 \end{pmatrix}_{\theta=13^\circ} \begin{pmatrix} x_b \\ y_b \end{pmatrix}$$

$$\begin{pmatrix} x_p \\ y_p \end{pmatrix} = \begin{pmatrix} -0.726 & -0.707 \\ -1.000 & 0.707 \end{pmatrix} \begin{pmatrix} x_b \\ y_b \end{pmatrix}$$

This 2 x 2 matrix is inverted to finally yield true beam position as a function of camera pixels.

$$\begin{pmatrix} x_b \\ y_b \end{pmatrix} = \begin{pmatrix} -0.579 & -0.579 \\ -1.000 & 0.707 \end{pmatrix} \begin{pmatrix} x_p \\ y_p \end{pmatrix}$$

Step 3.

Finally, a calibration of 32.5 px/mm is applied based upon independent calibration of ladder image to ladder motion (182.8 steps/mm).